




Random DFB-FL using apodized FBG and DFB-FL optical filters: a numerical performance evaluation

Ayman W. Elashmawy¹ · Hossam M. H. Shalaby¹ · Moustafa H. Aly² 

Received: 29 September 2021 / Accepted: 9 November 2021

© The Author(s), under exclusive licence to Springer Science+Business Media, LLC, part of Springer Nature 2021

Abstract

A random distributed feedback fiber laser (DFB-FL), with an apodized fiber Bragg grating (FBG) or an apodized Distributed feedback fiber (DFB) optical filter, is proposed. This leads to a narrow band light generation from the random DFB-FL optical source. This is a theoretical work depending in numerical analysis. Our proposed system consists of a random DFB-FL, with input pump power and long fiber length, followed by an optical filter. The filter has high reflectivity, high side lobe suppression ratio, and narrow full-width half-maximum (FWHM). A suitable apodization function is selected in order to improve the performance using the FBG/DFB optical filter. The performance of proposed system is evaluated by determining its reflectivity, SLSR, and FWHM over a 100 km random DFB-FL. Our results reveal that a FWHM of 0.09 nm with a high SLSR of 12.336 dB is achievable when using a Hamming apodization profile.

Keywords Apodization · Apodized DFB · Apodized FBG · FWHM · Random fiber laser · Reflectivity · SLSR

1 Introduction

Fiber lasers represent a motivating branch of light communication systems. Light that propagates through a fiber is enclosed inside a small medium of the core. Because of low loss, the propagation length is very large, which leads to accumulation of nonlinear effects. Amplification of light, by excited ions and atoms in active fibers or by Raman effect in non-active fibers, is combined with the nonlinear properties of the optical fiber to make the fiber laser very attractive in nonlinear processes' studies (Turitsyn et al. 2014).

The resonant cavity (or resonator) in classical laser science is the main element of the laser system which determines the emitted radiation properties. For example, the cavity

✉ Moustafa H. Aly
mosaly@aast.edu

¹ Electrical Engineering Departments, Faculty of Engineering, Alexandria University, Alexandria, Egypt

² Electronics and Communications Engineering Department, College of Engineering and Technology, Arab Academy for Science, Technology and Maritime Transport, Alexandria, Egypt

length determines the spacing between longitudinal modes and consequently, it determines the output frequency characteristics. Lasers having sub-micron cavity lengths are considered the shortest lasers, e.g., nanowire semiconductor lasers (Ma et al. 2013) and spacer-based nano-lasers (Ma and Oulton 2019). For fiber lasers, the cavity is generally formed by end reflectors inside the fiber such as fiber Bragg gratings (FBGs), which exhibits unique implementation stability. As a result of the excellent characteristics of the optical guiding concerning the low loss, the cavity lengths in fiber lasers can vary from small centimeters to multiples of hundreds of kilometers in ultra-long fiber lasers (Turitsyn et al. 2009). These lasers are used as light sources and as singular type of transmission media (Ania-Castañón et al. 2008). The long cavity length of a fiber laser, in addition to the broadening of the gain bandwidth of the doped fibers or/and Raman gain, assures that most of the longitudinal modes can be amplified, exist within the resonator, and coupled over the shared gain. Accordingly, fiber lasers can be operated in a high multimode system that has large nonlinear dynamic features.

The random laser concept (Mysliwiec et al. 2021) has been attracted lately for a great deal of concern, such as, simple technology providing compact design. This is because these lasers can generate coherent light without the traditional cavity through exploiting a multiple number of scatterings in a disordered amplified medium such as, active crystals powders or semiconductor particles. Various scattering types increase the path for an efficient amplification and provide a random feedback that results in lasing. The spatial and the spectral characteristics of the random laser output beam are obtained mainly by building up the radiation in extensive local or non-local spatial modes that are included randomly in the disordered bulk material.

The fiber refractive index has inhomogeneities. They are randomly distributed along the fiber. Rayleigh scattering (RS) within these inhomogeneities is the cause of setting loss limit at wavelengths near 1.55 μm , congruent to a transparent window of silica glasses that are the basic items in optical fiber communication systems (Agrawal 2010). The scattered radiation part of RS that is reflected to the fiber waveguide can be used for the purpose of feedback.

The back scattered radiation fraction is so small that it makes the total back scattered radiation within the fiber negligible even in a hundred kilometers long passive fiber. However, this situation is changed dramatically when the scattered radiation is amplified through Raman gain. This situation is the main difference from ordinary Raman fiber lasers having ordinary reflectors, even in ultra-long fiber cavities with lengths greater than 270 km (Turitsyn et al. 2009). Distributed random backscattering effects become comparable to regular feedback formed by the reflectors in the cavity placed at both fiber ends. The attempt to obtain RS based long fibers lasers without the regular reflectors has resulted in excellent output properties for a specific random laser, named as random distributed feedback fiber laser (DFB-FL) (Wang et al. 2018).

A laser is constructed using two main elements: a gain medium that provides an optical gain by means of stimulated emission and an optical cavity which traps the light partially in it. Random lasers work on the same principles, but the modes are determined by multiple scattering and not by a laser cavity. Recently, the random laser was demonstrated, that operates in a conventional telecommunication fiber without any resonator mirrors which is called random distributed feedback fiber laser (DFB-FL) (Agrawal 2010; Wang et al. 2018). The positive feedback which is required for laser generation in random fiber lasers is provided by Rayleigh scattering from the inhomogeneities of the refractive index that are already present in silica glass. In this type of lasers, the

randomly backscattered light is amplified through Raman effect and distributed gain over distances up to 100 km is provided.

Such a random DFB-FL has interesting and attractive features. The fiber waveguide geometry provides the transverse confinement, and leads to the generation of a stationary near-Gaussian beam with a narrow spectrum. It has efficiency and performance that are comparable to and even exceed those of similar conventional fiber lasers. In addition to its use in optical fiber communication systems, a range of other potential applications for random lasers include medical applications, compact light sources, monitoring devices, illumination materials and others.

Low-threshold power (~ 1 W), high efficiency (reaching 30%), a narrow band beam (around 1 nm), and a stable continuous wave (CW) of a near-Gaussian beam lasing at 1.55 μm has been achieved as in traditional telecom fiber having Raman gain, that is distributed homogeneously along the fiber long extent (Turitsyn et al. 2014). Due to the distributed gain and feedback, it is similar to ordinary distributed feedback fiber laser that uses the traditional FBGs permanently engraved in a few centimeters long heavily-doped active fibers with 180-degree phase shift formed at the middle. The random inhomogeneities of the fiber core refractive index represent the fingerprint of a particular fiber extent defined by fabrication and material imperfections. The light, which is scattered randomly, propagates in the amplifying medium within very complex paths (Turitsyn et al. 2014).

When pumping light of frequency ν_p is incident on a silica glass medium, it excites a quantum of molecular vibrations through an in-elastic scattering process, losing a small portion of its energy. Residual energy is carried out by a Stokes photon possessing a lower frequency, ν_s , than that of the pump photon. The difference in frequency between Stokes and pump photons is known as the Stokes shift, with a value obtained by a structure of vibrational levels in the host media. In a silica glass amorphous medium with different collective vibrations, Stokes photons of a wide range of energy following RS spectral profile could be emitted spontaneously. If there are some spontaneously scattered photons in the media, the stimulated RS could occur with a rate that depends on pump wave power, P_p , and the Stokes wave power, P_s (Turitsyn et al. 2014).

The obtained partial reflections are random in space and fully deterministic for both phase and amplitude in time, allowing coherent interference with each other. A single periodic grating engraved in a fiber amplifier is simply a conventional distributed feedback laser that generates a single longitudinal mode. Basically, the ordinary DFB fiber laser has a strong regular reflecting grating, while the random fiber laser has weak and extended random gratings. This gives the point that the mode in ordinary DFB fiber laser is mainly defined through the grating while the spatial power characteristics in the RS-based random fiber laser is mainly defined through its gain (Herrmann and Wilhelmi 1998).

The use of FBGs put requirements on the shape of the reflection spectrum, which is defined by the profile of the refractive index for the grating. One of the main common requirements is the suppression of side lobes. The absence of side lobes in FBG reflection spectra is achieved by apodization, which is varying the modulation amplitude smoothly and make an equalization for the average value of the induced refractive index through the grating. Apodization is the technique that weakens the secondary diffraction maxima, resulting in a suppression of the side lobes. A grating with a similar refractive modulation amplitude profile suppresses the side lobes substantially, making the reflection spectrum smooth, to achieve a narrower bandwidth which is the requirement for a good optical filter that can be used to obtain single output power from random DFB-FL (Kalimoldayev et al. 2019). Using apodized FBG or apodized DFB as an accurate C-band active optical filter that is proved by changing the apodization profile, will affect filter performance.

The major difference between the FBG and the DFB is that the FBG is without any gain in the grating. It is a passive device consisting of FBG for achieving the coupling between the incident and reflected waves. On the other hand, the DFB, which has the same structure of FBG, includes a gain medium that can achieve a gain for the reflected wave during the coupling. The required performance can be determined by careful selection of modulation depth and grating length according to WDM system filtering requirements (Nazmi et al. 2013, 2015).

A narrow-band emission with a spectral width down to ~ 0.05 nm linewidth is obtained in the random DFB-FL employing a narrow-band Gaussian apodized FBG filter or using optical fiber Fabry-Perot interferometer filters (Sugavanam et al. 2013). The fiber pigtailed tunable filter can be introduced in the middle of the scheme and using double source pumping to achieve spectral width ~ 1 nm (Babin et al. 2012). A widely tunable random fiber laser by using an Erbium Doped Fiber (EDF) as the gain media was used with a tunable optical fiber Fabry-Perot filter and random distributed feedback giving a narrow linewidth of about 0.04 nm (Wang et al. 2014). A linearly polarized Raman fiber laser with random DFB based on a polarization-maintaining twin-core fiber (TCF) was used to get a linewidth of about 0.5 nm that can be considered as five times smaller than that of random laser based on the ordinary fiber with same parameters (Budarnykh et al. 2018).

In this paper, we introduce a system that is consisting of random DFB-FL followed by an apodized FBG or DFB filter with different apodization profiles to test the performance of the random DFB-FL for the telecommunication applications. The reflectivity is a main parameter in the filter study. It also includes the region of the operating wavelengths. From the reflectivity, one can calculate the SLSR from the peak of the main lobe output and the peak of the highest side lobe in the region. Also, the FWHM indicates the region of wavelengths over which the reflectivity is high enough till the half power. The filter performance is chosen with high SLSR and narrow bandwidth that can be used in WDM systems.

For each profile, we examine the reflectivity spectrum concerning the maximum reflectivity, FWHM, and SLSR in order to obtain the best apodization profile for either FBG or DFB to get a nearly single wavelength output from the random DFB-FL that is essential for WDM communication systems. This work considers only the RS nonlinearity in the random laser, with performance comparison using both apodized FBG and apodized DFB filters.

The reflectivity means the ratio between the reflected power and the incident power to the optical filter. The FBG and the DFB are based on the principle of the Bragg grating which reflects the wave with the desired wavelength. High reflectivity means high reflected power is obtained at the output of the filter. So, reflectivity spectrum is an indicator of the output of the DFB-FL.

The remainder of this paper is organized as follows. The mathematical model upon which simulations are based is presented in Sect. 2, including the apodization functions used in this paper. The system under study is illustrated and explained in Sect. 3. The obtained results for various apodization profiles are reported and discussed in Sect. 4. We summarize and conclude the obtained results in Sect. 5.

2 Model and analysis

In this section, we present the mathematical model used to get the reflectivity and output power for the cases of DFB laser and FBG following random DFB-FL.

Our model starts with the power balance equations that describe performance of the DFB random laser. The conditions are introduced for the case of single arm pumping in addition to the equations used for the threshold power calculation, amplification length as well as the effect of the parasitic reflections at both random DFB laser ends. After that, it is necessary to describe the coupled mode equations for single mode FBG operation. To describe the performance of the DFB F-FL, the effect of the gain of the active medium is introduced generating coupled mode equations for the DFB-FL.

Using coupled mode equations, one can solve using the boundary conditions for the stage of the DFB-FL to get forward and backward waves. After that, we can get the reflection coefficient thus obtaining the reflectivity. This is carried out for the case of uniform FBG, apodized FBG with different apodization profiles, the uniform case of the DFB-FL and then for apodized DFB profiles assuming a gain in the active medium just below the threshold value for the case of uniform structure.

2.1 Analysis sequence

Figure 1 illustrates the analysis sequence. The coupled mode equations are then applied to the apodized DFB-FL section knowing the apodization profile, length of the grating, and the degree of coupling obtaining the reflected wave distribution, forward wave distribution, and the reflectivity. The evaluation parameters of the optical filter include Side Lobe Suppression Ratio (SLSR), Full Wave Half Maximum (FWHM), filter gain, and reflectivity.

2.2 Power balance equations for the random DFB-FL

The power balance technique is based on the system of equations concerning the average power performance. The technique considers the material effects, such as loss in fiber, Raman gain, amplified spontaneous emission (ASE), Rayleigh backscattering and the effect

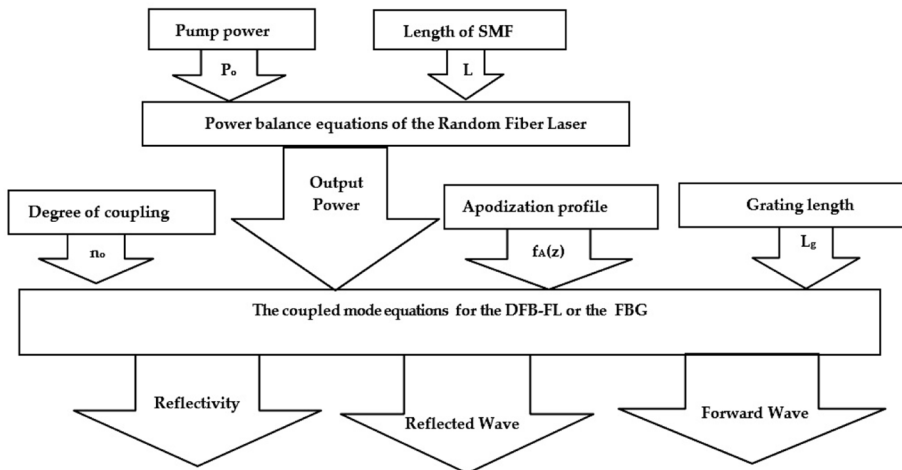


Fig. 1 Analysis sequence flow chart

of travelling through fiber. This technique is better used for describing the performance of the random DFB-FLs. One can apply the power balance model to explain the effect of RS on lasing.

A narrow signal laser system, at a single pump wavelength, generated from the pump waves, is represented by Turitsyn et al. (2014); Lin et al. (2020):

$$\frac{dP}{dz} = -\alpha_P P_P - g_R \frac{\nu_P}{\nu_S} P_P (P_S^- + P_S^+ + 4h\nu_S \Delta\nu) \tag{1.a}$$

$$\frac{dP_S^+}{dz} = -\alpha_S P_S^+ + g_R P_P (P_S^+ + 2h\nu_S \Delta\nu) + \epsilon P_S^- \tag{1.b}$$

$$\frac{dP_S^-}{dz} = \alpha_S P_S^- - g_R P_P (P_S^- + 2h\nu_S \Delta\nu) - \epsilon P_S^+ \tag{1.c}$$

where P_P, P_S are pump and first Stokes wave powers, respectively, $\nu_{s,p}$ are Stokes and pump waves frequencies, respectively, $\alpha_{s,p}$ are fiber losses at pump and signal frequencies, respectively, g_R is Raman gain coefficient, while ϵ is the Rayleigh scattering coefficients, at Stokes wave frequency. The Rayleigh parameter ϵ is defined as $\epsilon = \alpha_S Q$ where Q is the factor of geometry (Brinkmeyer 1980), considering the fraction of the scattered radiation which is regained by the fiber. The numerical value of the Rayleigh parameter depends on the fiber numerical aperture and its fabrication (Bisyarin et al. 2017a, 2017b). Although the parameter ϵ is very small, the Rayleigh backscattering has a major effect for the random fiber lasers.

The term $h\nu_S \Delta\nu$ represents the spontaneous RS, where $\Delta\nu$ is the Raman gain spectral width. The term representing spontaneous RS is small as compared to other terms, however, it has an appreciable role, in order for the equations do not have no solution in the numerical simulations.

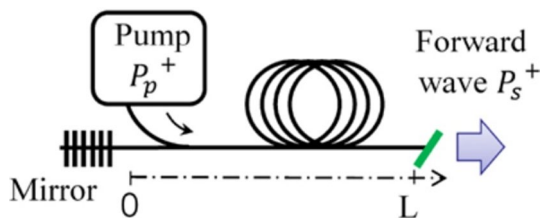
The value for the Raman gain, g_R , which is independent of wavelength is considered at the maximum Raman gain spectral profile. The Raman gain normal width is approximately 10 nm, while that for the generation spectrum in random DFB-FL is approximately 1 nm (Turitsyn et al. 2014).

For the case under consideration, it is called forward-pumped configuration shown in Fig. 2.

As shown in Fig. 2, one fiber end, $z = L$, has no reflection and at other end, $z = 0$, there is a full reflection for the ideal case. But, there is a parasitic reflection due to the surface scattering at both fiber ends which modify the boundary conditions to be as follows

$$P_S^-(0) = R_F P_S^+(0), \quad P_S^-(L) = R_F P_S^+(L), \quad P_P(0) = P_O \tag{2}$$

Fig. 2 Random DFB-FL forward pumped configuration



where P_O is the input pump power, R_L and R_F are the parasitic reflection due to the surface scattering at both fiber ends, with the numerical values of 1.5×10^{-3} and 2×10^{-4} , respectively (Sugavanam et al. 2013).

To solve Eq. (1) numerically using MATLAB 2017, one can input the pump power and the length of the fiber for the random DFB-FL, solving the equations to get the output power that will be input to the filter section which consists of FBG-FL or DFB-FL filter which could be uniform or apodized.

2.3 Coupled mode equations for DFB and FBG

The coupled mode theory is used to analyze the behavior of simple DFB lasers (Wonga et al. 2011). A schematic of coupling between forward and backward waves is shown in Fig. 3, for waveguides having periodic refractive index modulation, like FBG, where the core refractive index varies according to a certain apodization profile.

The coupled wave equations for a DFB-FL are given by Zhao et al. (2011):

$$\frac{dR(z)}{dz} = \left(g - j\delta + \frac{1}{2} \frac{d\Phi(z)}{dz} \right) R(z) - j\kappa S(z) \tag{3.a}$$

$$\frac{dS(z)}{dz} = \left(g - j\delta + \frac{1}{2} \frac{d\Phi(z)}{dz} \right) S(z) + j\kappa R(z) \tag{3.b}$$

$$\delta = \beta - \beta_D = 2\pi n_{eff} \left(\frac{1}{\lambda} - \frac{1}{\lambda_D} \right) \tag{4}$$

$$\kappa = \frac{\pi}{\lambda} n_o f_A(z) \tag{5}$$

where g is the DFB active region gain per unit length, δ is the grating detuning, n_{eff} is the fiber core effective refractive index, λ is the incoming signal wavelength, λ_D is the designed filter wavelength, κ is the coupling coefficient between the forward and backward waves, $L = L_g$ is the length of grating, $\Phi(z)$ is the wave phase, n_o is modulation depth, and $f_A(z)$ represents the apodization profile function. The parameter κ represents the coupling coefficient between the incident and reflected waves inside the grating region of the FBG and DFB-FL. The coupling coefficient depends on the modulation depth (degree of coupling) and the apodization function. Large coupling coefficient indicates a high coupling between the incident power to the reflected power.

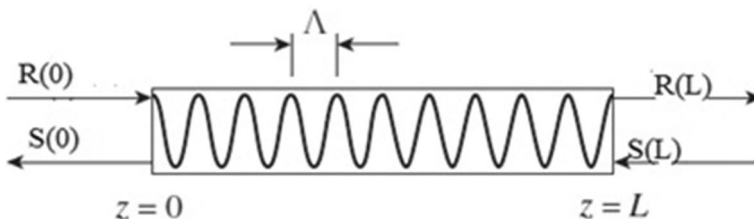


Fig. 3 Forward and backward waves in periodic active waveguides

In the analysis, it is assumed that there is no grating chirp i.e. $(\frac{d\Phi(z)}{dz} = 0)$ and the gain is constant value, which must be below the threshold value in order to avoid lasing and to operate as an optical filter. The gain is given by $g = 0.98g_{th}$, as case of the uniform DFB-FL to avoid lasing of the DFB-FL and to operate as an optical filter, where g_{th} is the threshold gain given by Nazmi et al. (2015)

$$g_{th} = 4\kappa_m e^{-\kappa_m L_g} + \alpha_s \tag{6}$$

where κ_m represents the value of the coupling coefficient for the case of uniform DFB-FL and α_s is the back-ground loss of the used fiber.

Many apodization functions can be used to enhance the characteristics of the DFB/FBG as an optical filter. In this paper, we use the following apodization functions for a FBG/DFB of length L_g (Sayed et al. 2020).

- (1) Uniform

$$f_A(z) = 1, 0 \leq z \leq L_g \tag{7}$$

- (2) Hamming

$$f_A(z) = \left[\frac{1 + H \cos\left(\frac{2\pi(z - \frac{L_g}{2})}{L_g}\right)}{1 + H} \right], 0 \leq z \leq L_g \tag{8}$$

where $H = 0.665$,

- (3) Gaussian

$$f_A(z) = \exp\left(-a\left(\frac{z}{L_g} - 0.5\right)^2\right), 0 \leq z \leq L_g \tag{9}$$

where $a = 4$,

- (4) Raised Cosine

$$f_A(z) = \sin^2\left(\frac{\pi z}{L_g}\right), 0 \leq z \leq L_g \tag{10}$$

- (5) Positive- tanh

$$f_A(z) = \begin{cases} \tanh\left(\frac{2s z}{L_g}\right), 0 \leq z \leq \frac{L_g}{2} \\ \tanh\left(\frac{2s(L_g - z)}{L_g}\right), \frac{L_g}{2} \leq z \leq L_g \end{cases} \tag{11}$$

where $s = 4$.

3 The proposed system

The system under study is simulated with MATLAB. An apodized FBG/DFB is used with various apodization profiles after the random DFB-FL for the ease of filtering. The system is illustrated in Fig. 4. The system is shown only for the ease of description in Fig. 4. The system and the FBG/DFB parameters, used in simulations, are summarized in Tables 1 and 2, respectively.

The wavelength 1550 nm is preferable for optical communication systems, which corresponds to minimum dispersion and minimum attenuation. The minimum dispersion leads to higher bit rates, while the minimum attenuation leads to larger transmission distances and reduces the number of optical amplifiers in the optical fiber communication system.

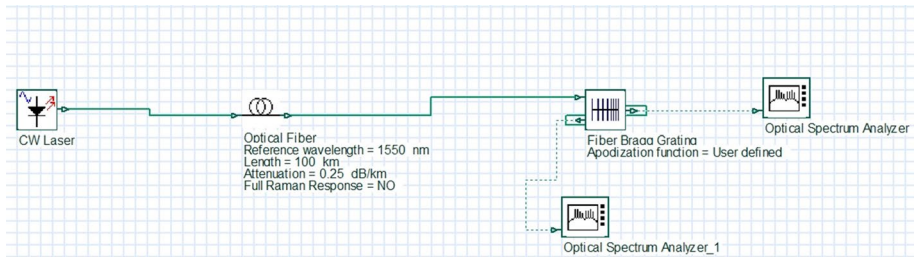


Fig. 4 The proposed system of random DFB-FL followed by FBG/DFB filter

Table 1 Random DFB-FL parameters (Turitsyn et al. 2014; Nazmi et al. 2015; Sugavanam et al. 2013; Vatnik et al. 2012)

DFB-FL Parameters	Value
Pump power (W)	1
Parasitic reflection due to the surface scattering at both fiber ends	1.5×10^{-3} and 2×10^{-4}
Raman gain coefficient ($W^{-1} km^{-1}$)	0.39
Attenuation of the fiber at the pump frequency (km^{-1})	0.055
Attenuation of the fiber at the signal frequency (km^{-1})	0.045
Fiber length (km)	100
Pump wave wavelength (nm)	1455
Raman gain spectral profile width (nm)	10
Geometrical factor	0.001

Table 2 FBG/DFB parameters (Turitsyn et al. 2014; Nazmi et al. 2015; Sugavanam et al. 2013; Vatnik et al. 2012)

Parameter	Value
Grating length	5, 10, 20 mm
Reference wavelength	1550 nm
Effective refractive index	1.47
Refractive index modulation depth	$10^{-3}, 10^{-4}, 10^{-5}$
Back ground loss	$0.15 m^{-1}$

i. *The Random DFB-FL*

A laser source is used as a pump signal to the random fiber laser. The CW laser source frequency is 206.9 THz ($\lambda = 1450$ nm) with an output power of 1 W. This pump light is incident on a random DFB-FL medium. The fiber is 100 km long with 0.25 dB/km attenuation, and full Raman spectral response.

ii. *The FBG/DFB filter*

In FBG design, apodization is used for the purpose of narrowing spectral responses, compressing side lobes and improving dispersion compensation of chirped grating (Sayed et al. 2020). However, the effects of apodization in DFB-FL are not widely explored especially in analysing the performance parameters such as output power, line width, amplitude and phase noise, as well as stability of single longitudinal mode operation.

The output power of the apodized FBG/DFB is strongly dependent on the apodization profile shape and the effective grating strength. Understanding the apodization effects on system performance is useful to design a DFB-FL with optimized bidirectional or unidirectional output power (Nazmi et al. 2015).

The FBG/DFB is apodized using main apodization profiles in addition to the uniform profile. We study the performance of the output of the FBG/DFB filter designed at 1550 nm concerning the reflectivity, SLSR, and FWHM.

4 Results and discussion

The variation in modulation depth of the apodized FBG/DFB optical filter will cause the reflectivity spectrum to change its response. Figure 5 shows the reflectivity spectrum for the case of Hamming apodized FBG filter for modulation depths of 10^{-3} (strong modulation), 10^{-4} (moderate modulation), and 10^{-5} (weak modulation). As shown in Fig. 5, the strong modulation gives the highest reflectivity but with very large side lobes that cannot be accepted. While the moderate modulation gives an acceptable reflectivity and low side lobes, and the weak modulation gives a very poor reflectivity that cannot be accepted. Thus, the incoming simulations will be based on the moderate modulation depth (10^{-4}).

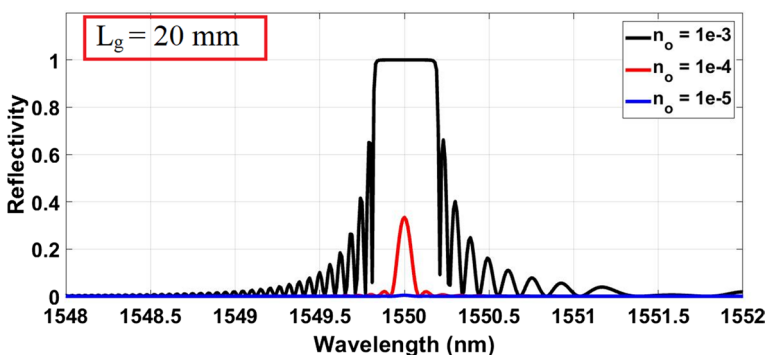


Fig. 5 Effect of modulation depth variation in case of Hamming FBG apodization on reflectivity spectrum at constant grating length

The length of the grating in the apodized FBG/DFB optical filter also affects the reflectivity spectrum. Figure 6 shows the effect of the grating length on the reflectivity spectrum at the moderate modulation of 10^{-4} . As shown in Fig. 6, the large grating length of 20 mm achieves the highest reflectivity and the best FWHM, while the other two grating lengths of 10 mm and 5 mm give lower reflectivity and wider bandwidth. So, the grating length used in the incoming simulations is chosen as the larger grating length of value 20 mm.

Based on the described model, we present the obtained results including FBG/DFB reflectivity, SLSR, and FWHM for each apodization function. There must be a compromise in the requirements for best case concerning the maximum reflectivity, SLSR and FWHM. One needs high reflectivity, very high SLSR and very narrow FWHM. To achieve our requirements, simulations are made for different grating length values. It is found that at large grating length (20 mm), the reflectivity is very high compared to other lengths, with an accepted value of SLSR. Also, the FWHM is narrower than that achieved by shorter grating lengths. Accordingly, larger grating lengths are recommended.

4.1 Reflectivity

The reflectivity of the FBG/DFB of each apodization function are illustrated in Fig. 7a-j for the best grating length and modulation depth that can achieve the requirements for a selective filter. The reflectivity shows the reflected wavelength band which can be compensated using the apodized FBG/DFB in the C-band range.

In Fig. 7, the reflectivity of the DFB Gaussian and raised cosine apodization profiles are the same and shifted to a higher wavelength (1552.7 nm) giving zero reflectivity at 1550 nm. Also, the reflectivity of the FBG for the same profiles are shifted to lower wavelength (1547.1 nm) and give the same reflectivity.

The reflectivity of the positive-tanh apodization is similar to that of the uniform apodization for the case of both FBG/DFB filters. A very small reflectivity is noticed in the Gaussian and raised cosine profiles, and a relatively large reflectivity for the case of the positive-tanh and uniform apodization profiles.

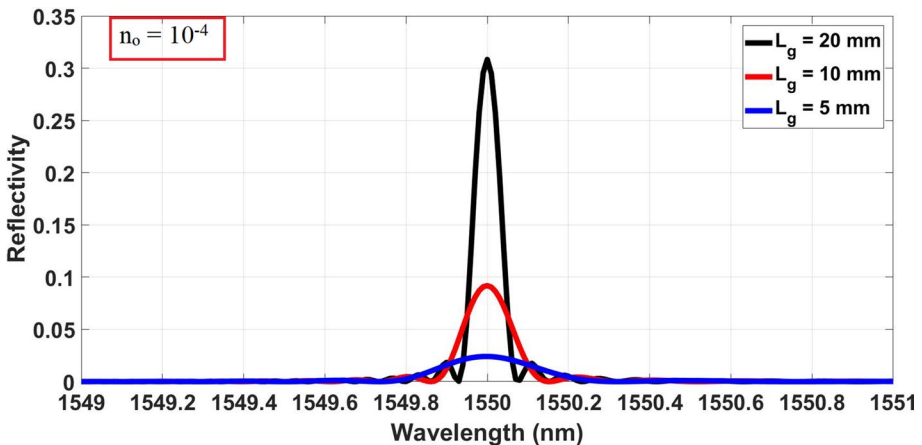


Fig. 6 Effect of grating length variation on reflectivity spectrum for the case of Hamming FBG apodization at constant modulation depth

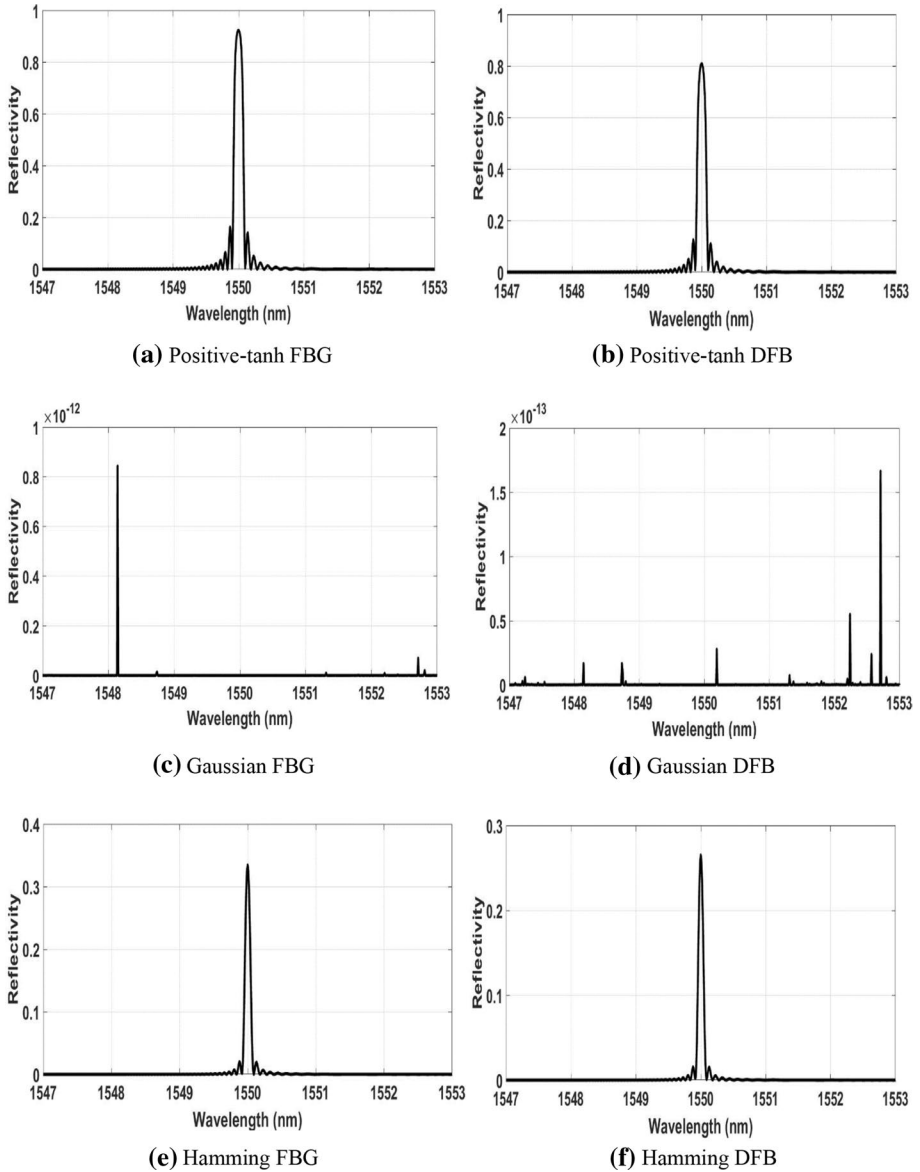


Fig. 7 Reflectivity for each apodization profile with FBG and DFB

The Hamming profile has moderate reflectivity and smaller side lobes. Small ripples are noticed for the side lobes in all cases except for the Gaussian and raised cosine profiles.

It is noticed that the reflectivity for the case of FBG is higher than that of the DFB case. Different profiles but with the same behavior achieve the same reflectivity as shown in the Gaussian and raised cosine cases, also for the positive-tanh and uniform cases. Table 3 summarizes the values of the maximum reflectivity for various apodization function profiles.

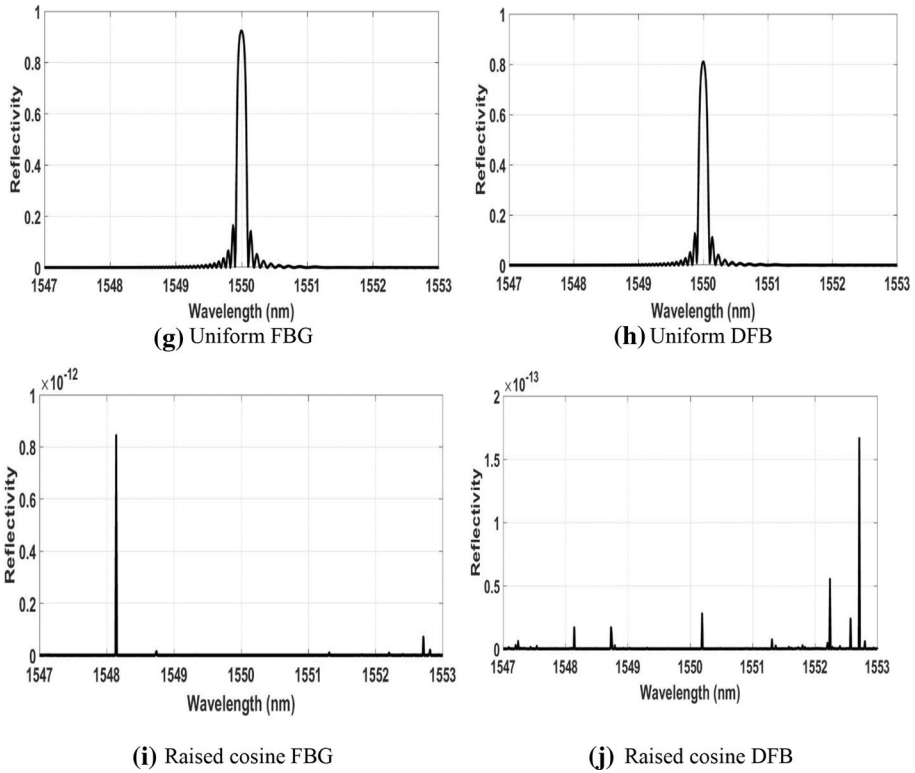


Fig. 7 (continued)

Table 3 Reflectivity for the apodization function profiles

Apodization function profile	Reflectivity
FBG positive-tanh	0.9239
DFB positive-tanh	0.8099
FBG Gaussian	8.439×10^{-13}
DFB Gaussian	1.665×10^{-13}
FBG Hamming	0.3346
DFB Hamming	0.2652
FBG uniform	0.9239
DFB uniform	0.8099
FBG raised cosine	8.439×10^{-13}
DFB raised cosine	1.665×10^{-13}

4.2 FWHM ($\Delta\lambda$)

Figure 8 shows the 3-dB bandwidth in the Hamming FBG reflectivity, that gives the FWHM which represents the selectivity for the apodized FBG/DFB filters.

As shown in Fig. 8, the maximum reflectivity is 0.3346 at 1550 nm wavelength, while half of the maximum is 0.1673 and occurs at the reflectivity curve giving a wavelength range

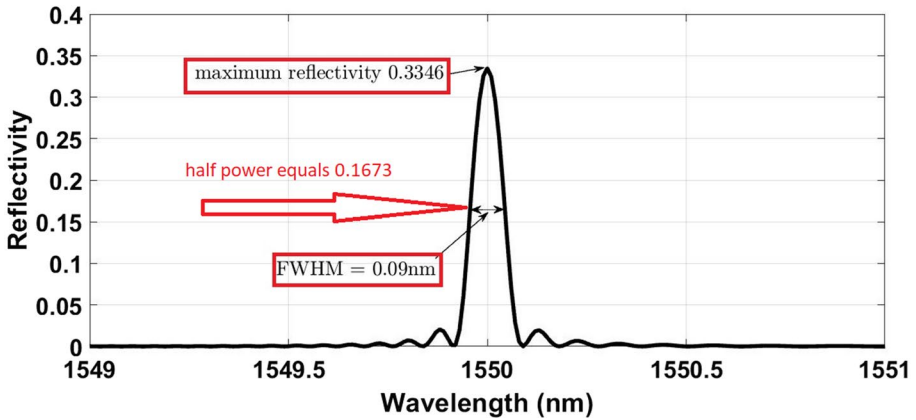


Fig. 8 FWHM ($\Delta\lambda$) for the Hamming FBG apodized filter

approximately 0.09 nm. The other FWHM can be obtained by repeating the procedure and the results are summarized in Table 4.

As shown in Table 4, uniform and positive-tanh profiles show the same and the largest bandwidth, 0.16 nm. The Gaussian and raised cosine profiles are the same giving the narrower bandwidth of 0.02 nm making them the most selected filters. The Hamming profile gives a bandwidth of 0.09 nm which makes it more selected than uniform and positive-tanh profiles. From the obtained results, the most selected filters are the filters having Gaussian and raised cosine apodization profiles for both cases of FBG and DFB

4.3 SLSR

The SLSR can be calculated knowing the values of maximum reflectivity and maximum side lobe in the spectrum using

$$SLSR = 10\log\left(\frac{\text{maximum reflectivity}}{\text{maximum side lobe value}}\right) \tag{12}$$

Table 4 FWHM ($\Delta\lambda$) for the apodization profile functions

Type	Apodization profile	FWHM (nm)
FBG	Positive-tanh	0.16
	Gaussian	0.02
	Hamming	0.09
	Uniform	0.16
	Raised cosine	0.02
DFB	Positive-tanh	0.16
	Gaussian	0.02
	Hamming	0.09
	Uniform	0.16
	Raised cosine	0.02

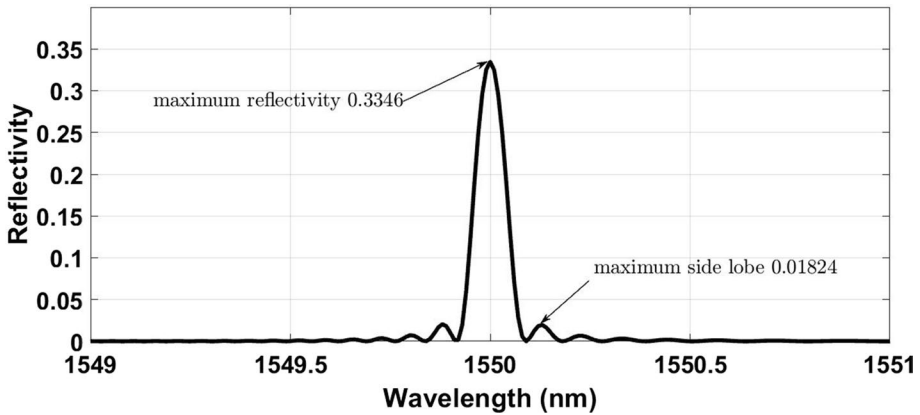


Fig. 9 SLSR calculation using Hamming FBG apodized filter

Table 5 SLSR for various apodization profile functions

Type	Apodization profile	SLSR (dB)
FBG	Positive-tanh	7.53
	Gaussian	10.8
	Hamming	12.336
	Uniform	7.518
	Raised cosine	10.8
DFB	Positive-tanh	8.08
	Gaussian	4.8034
	Hamming	12.377
	Uniform	8.08
	Raised cosine	4.8

Figure 9 displays the side lobes for the Hamming FBG reflectivity, that is used in calculating the SLSR that represents the degree of single reflected wavelength operation using the apodized FBG/DFB filters. As shown, the maximum reflectivity is 0.3346, while the maximum side lobe value is 0.01824 at the reflectivity curve giving a SLSR of 12.336 dB. The other SLSR for different apodization profiles are obtained by a similar approach and the results are summarized in Table 5.

As shown in Table 5, the FBG and DFB profiles give different values of SLSR. However, the profiles having the same behavior give the same SLSR as the case of positive-tanh and uniform profiles, and nearly equal in cases of Gaussian and raised cosine profiles. The DFB and FBG Hamming apodization profile gives the highest SLSR of 12.377 dB and 12.336 dB, respectively, that makes this profile the best choice in suppressing the side lobes and gives nearly a single reflected wavelength. The DFB raised cosine gives the smallest SLSR that means not a single reflected wavelength.

5 Summary

Table 6 summarizes the obtained results for the different apodization profiles for both FBG and DFB constructions that can be useful in analyzing the performance for the filters and choosing the best design that achieves the requirements of higher reflectivity, narrow FWHM, and high SLSR.

As shown in Table 6, the raised cosine and the Gaussian profiles give better selectivity for the filter and a good SLSR but with very small reflectivity that is nearly zero. Also, the shifted reflectivity spectrum at wavelengths other than 1550 nm makes them a bad choice.

The uniform and the positive-tanh profiles achieve high reflectivity and acceptable SLSR with wider bandwidth that means less selectivity for the filter. This is useful in applications that need high reflectivity with no concern on the bandwidth.

The Hamming profile with both FBG and DFB constructions achieve the highest SLSR. Thus, higher suppression for side lobes and nearly single reflected wavelength, reflectivity spectrum centered at the required wavelength of 1550 nm, makes this filter be considered as a narrow bandwidth one that can be used in applications that require high selectivity. However, the reflectivity is not high but could be acceptable.

The SLSR value of the Hamming profile is not very large, but this value is the highest among the apodization profiles under the case study giving a better performance for the system but there can be another apodization profiles not taken in to consideration that can give higher SLSR. The SLSR value of the Hamming profile is not very large, but this value is the highest among the apodization profiles under the case study giving a better performance for the system.

6 Conclusion

In this paper, a system containing the random DFB-FL followed by an apodized FBG/DFB filter is proposed and simulated using different apodization profiles. The filter performance is chosen with higher reflectivity, high SLSR, and narrow bandwidth that can be used in WDM systems. Simulation results revealed that according to the required application, a trade-off study is required to choose the best apodization profile according to application. But, overall, the FBG Hamming apodized filter achieves the most

Table 6 Summary for the different apodization profiles

Type	Apodization	Reflectivity	FWHM	SLSR
FBG	Positive-tanh	0.9239	0.16 nm	7.53 dB
	Gaussian	8.439×10^{-3}	0.02 nm	10.8 dB
	Hamming	0.3346	0.09 nm	12.336 dB
	Uniform	0.9239	0.16 nm	7.518 dB
	Raised cosine	8.439×10^{-3}	0.02 nm	10.8 dB
DFB	Positive-tanh	0.8099	0.16 nm	8.08 dB
	Gaussian	1.665×10^{-3}	0.02 nm	4.8034 dB
	Hamming	0.2652	0.09 nm	12.377 dB
	Uniform	0.8099	0.16 nm	8.08 dB
	Raised cosine	1.665×10^{-13}	0.02 nm	4.8 dB

preferable response with moderate reflectivity (0.3346), spectrum at our concern wavelength of 1550 nm, high SLSR (12.336 dB), and narrow bandwidth (0.09 nm).

References

- Agrawal, G.P.: Fiber-optic communication systems. Wiley, USA (2010)
- Ania-Castañón, J.D., Karalekas, V., Harper, P., Turitsyn, S.K.: Simultaneous spatial and spectral transparency in ultra-long fiber lasers. *Phys. Rev. Lett.* **101**(12), 123903 (2008)
- Babin, S. A., El-Taher, A. E., Harper, P., Podivilov, E. V., and Turitsyn, S. K. (2012) "Broadly tunable high-power random fiber laser", in *SPIE Proc., Fiber Lasers IX: Technology. Syst Appl* 54: 82373E1–82373E9
- Bisyarin, M.A., Kotov, O.I., Hartog, A.H., Liokumovich, L.B., Ushakov, N.A.: Influence of a variable Rayleigh scattering-loss coefficient on the light backscattering in multimode optical fibers. *Appl. Opt.* **56**(16), 4629–4635 (2017a)
- Bisyarin, M.A., Kotov, O.I., Hartog, A.H., Liokumovich, L.B., Ushakov, N.A.: Rayleigh backscattering from the fundamental mode in step-index multimode optical fibers. *Appl. Opt.* **56**(2), 354–364 (2017b)
- Brinkmeyer, E.: Analysis of the back-scattering method for single-mode optical fibers. *J. Opt. Soc. Am.* **70**(8), 1010–1012 (1980)
- Budarnykh, A.E., Lobach, I.A., Zlobina, E.A., Velmiskin, V.V., Kablukov, S.I., Semjonov, S.L., Babin, S.A.: Raman fiber laser with random distributed feedback based on a twin-core fiber. *Opt. Lett.* **43**(3), 567–570 (2018)
- Herrmann, J., Wilhelmi, B.: Mirrorless laser action by randomly distributed feedback in amplifying disordered media with scattering centers. *Appl. Phys. B* **66**(3), 305–312 (1998)
- Kalimoldayev, M., Kalizhanova, A., Wójcik, W., Kashaganova, G., Amirgaliyeva, S., Dasibekov, A., Kozbakova, A., and Aitkulov, Z., "Research of the Spectral Characteristics of Apodized Fiber Bragg Gratings", in 2019 24th International Conference on Applied Mathematics, Computational Science and Systems Engineering, ITM Web Conference, 01015, AMCSE 2018, 2019.
- Lin, S., Wang, Z., Araújo, H.A., Raposo, E.P., Gomes, A.S.L., Wu, H., Fan, M., Rao, Y.: Ultrafast convergent power-balance model for Raman random fiber laser with half-open cavity". *Opt. Expr.* **28**(15), 22500–22510 (2020)
- Ma, R.M., Oulton, R.F.: Applications of nanolasers. *Nature Nanotech.* **14**(1), 12–22 (2019)
- Ma, Y., Guo, X., Wu, X., Dai, L., Tong, L.: Semiconductor nanowire lasers. *Adv. Opt. Photonics.* **5**(3), 216–273 (2013)
- Mysliwiec, J., Szukalska, A., Szukaski, A., Sznitko, L.: Liquid crystal lasers: the last decade and the future. *Nanophotonics.* **10**(9), 2309–2346 (2021)
- Nazmi, A.M., Elashmawy, A.W., Aly, M.H.: Apodized distributed feedback fiber laser as an optical filter. *J. Mod. Opt.* **60**(20), 1701–1712 (2013)
- Nazmi, A.M., Elashmawy, A.W., Aly, M.H.: Distributed feedback fiber filter based on apodized fiber Bragg grating. *Optoelectron. Adv. Mater. - Rapid Commun.* **9**(9–10), 1093–1099 (2015)
- Sayed, A., Mustfa, F.M., Khalaf, A.A.M., Aly, M.H.: Apodized chirped fiber Bragg grating for post dispersion compensation in wavelength division multiplexing optical networks. *Int. J. Commun. Syst.* **33**(2), 4551–4564 (2020)
- Sugavanam, S., Tarasov, N., Shu, X., Churkin, D.V.: Narrow-band generation in random distributed feedback fiber laser. *Opt. Expr.* **21**(14), 16466–16472 (2013)
- Turitsyn, S.K., Ania-Castañón, J.D., Babin, S.A., Karalekas, V., Harper, P., Churkin, D., Kablukov, S.I., El-Taher, A.E., Podivilov, E.V., Mezentsev, V.K.: "270-km ultra-long Raman fiber laser." *Phys Rev Lett* **103**(13), 133901 (2009)
- Turitsyn, S.K., Babin, S.A., Churkin, D.V., Vatnik, I.D., Nikulin, M., Podivilov, E.V.: Random distributed feedback fibre lasers. *Phys. Rep.* **542**(2), 133–193 (2014)
- Vatnik, I.D., Churkin, D.V., Babin, S.A.: Power optimization of random distributed feedback fiber lasers. *Opt. Expr.* **20**(27), 28033–28038 (2012)
- Wang, L., Dong, X., Shum, P.P., Su, H.: Tunable erbium-doped fiber laser based on random distributed feedback. *IEEE Photonics J.* **6**(5), 1–5 (2014)
- Wang, X., Chen, D., Li, H., She, L., Wu, Q.: Random fiber laser based on artificially controlled backscattering fibers. *Appl. Opt.* **57**(2), 258–262 (2018)

- Wonga, A.C.L., Chungb, W.H., Tamb, H.Y., Lua, C.: Ultra-short distributed feedback fiber laser with sub-kilohertz linewidth for sensing applications. *Laser Phys.* **21**(1), 163–168 (2011)
- Zhao, Y., Wang, Q., Chang, J., Ni, J., and Wang, Z., “Single polarization output of erbium-doped DFB fiber laser by self-injection locking”, in 2011 4th Proc. of International Conference on Electronics and Optoelectronics (ICEOE 2011), Dalian, Liaoning, China, pp. 454–456, July 2011.

Publisher's Note Springer Nature remains neutral with regard to jurisdictional claims in published maps and institutional affiliations.